



Research paper

GSTM3 variant is a novel genetic modifier in Brugada syndrome, a disease with risk of sudden cardiac death



Jyh-Ming Jimmy Juang^a, Anna Binda^b, Shyh-Jye Lee^c, Juey-Jen Hwang^a, Wen-Jone Chen^a, Yen-Bin Liu^a, Lian-Yu Lin^a, Chih-Chieh Yu^a, Li-Ting Ho^a, Hui-Chun Huang^a, Ching-Yu Julius Chen^a, Tzu-Pin Lu^{d,e,*}, Liang-Chuan Lai^f, Shih-Fan Sherri Yeh^g, Ling-Ping Lai^a, Eric Y. Chuang^h, Ilaria Rivolta^b, Charles Antzelevitch^{i,**}

^a Cardiovascular Center and Division of Cardiology, Department of Internal Medicine, National Taiwan University Hospital and National Taiwan University College of Medicine, Taipei, Taiwan

^b University of Milano Bicocca School of Medicine and Surgery, Via Cadore, 48, 20900 Monza (MB), Italy

^c Department of Life Science, National Taiwan University, Taipei, Taiwan

^d Institute of Epidemiology and Preventive Medicine, National Taiwan University, Taipei, Taiwan

^e Department of Public Health, National Taiwan University, Taipei, Taiwan

^f Graduate Institute of Physiology, National Taiwan University, Taipei, Taiwan

^g Department of Environmental and Occupational Medicine, National Taiwan University Hospital, Hsin-Chu branch and National Taiwan University College of Medicine, Taipei, Taiwan

^h Graduate Institute of Biomedical Electronics and Bioinformatics, National Taiwan University, Taipei, Taiwan

ⁱ Lankenau Institute for Medical Research and Lankenau Heart Institute, Wynnewood, PA and Sidney Kimmel Medical College of Thomas Jefferson University, Philadelphia, PA, USA

ARTICLE INFO

Article History:

Received 11 March 2020

Revised 28 May 2020

Accepted 3 June 2020

Available online xxx

Keywords:

Inherited cardiac arrhythmia

Genetics

Sudden cardiac death

Brugada syndrome

ABSTRACT

Background: Brugada syndrome (BrS) is a rare inherited disease causing sudden cardiac death (SCD). Copy number variants (CNVs) can contribute to disease susceptibility, but their role in Brugada syndrome (BrS) is unknown. We aimed to identify a CNV associated with BrS and elucidated its clinical implications.

Methods: We enrolled 335 unrelated BrS patients from 2000 to 2018 in the Taiwanese population. Microarray and exome sequencing were used for discovery phase whereas Sanger sequencing was used for the validation phase. HEK cells and zebrafish were used to characterize the function of the CNV variant.

Findings: A copy number deletion of *GSTM3* (chr1:109737011-109737301, hg38) containing the eighth exon and the transcription stop codon was observed in 23.9% of BrS patients versus 0.8% of 15,829 controls in Taiwan Biobank ($P < 0.001$), and 0% in gnomAD. Co-segregation analysis showed that the co-segregation rate was 20%. Patch clamp experiments showed that in an oxidative stress environment, *GSTM3* down-regulation leads to a significant decrease of cardiac sodium channel current amplitude. Ventricular arrhythmia incidence was significantly greater in *gstm3* knockout zebrafish at baseline and after flecainide, but was reduced after quinidine, consistent with clinical observations. BrS patients carrying the *GSTM3* deletion had higher rates of sudden cardiac arrest and syncope compared to those without (OR: 3.18 (1.77–5.74), $P < 0.001$; OR: 1.76 (1.02–3.05), $P = 0.04$, respectively).

Interpretation: This *GSTM3* deletion is frequently observed in BrS patients and is associated with reduced I_{Na} , pointing to this as a novel potential genetic modifier/risk predictor for the development of the electrocardiographic and arrhythmic manifestations of BrS.

Funding: This work was supported by the Ministry of Science and Technology (107-2314-B-002-261-MY3 to J.M.J. Juang), and by grants HL47678, HL138103 and HL152201 from the National Institutes of Health to CA.

© 2020 The Authors. Published by Elsevier B.V. This is an open access article under the CC BY-NC-ND license. (<http://creativecommons.org/licenses/by-nc-nd/4.0/>)

The abstract of this study was presented in 2018 ESC congress (EUD ID:787184) at Munich, Germany*

* Corresponding author at: Institute of Epidemiology and Preventive Medicine, National Taiwan University, Taipei, Taiwan.

** Corresponding author.

E-mail addresses: tplu@ntu.edu.tw (T.-P. Lu), antzelevitch@mlhs.org (C. Antzelevitch).

1. Introduction

Brugada Syndrome (BrS) is a cardiac channelopathy associated with an increased risk of sudden death. The prevalence of BrS is estimated to be 1–5 per 10,000 people in Caucasians but is higher in

Research in Context section

Evidence before this study

Unexpected sudden cardiac death in the young (SCDY) always make people, especially parents, grieve over their lost tremendously. Brugada Syndrome (BrS) is one of SCDY, an inheritable cardiac channelopathy associated with an increased risk of young sudden death or syncope, and a distinct electrocardiogram (ECG) pattern consisting of a right bundle-branch block with ST segment elevation in V1, and V2 in the absence of any structural heart disease. The average age at diagnosis is 40 ± 22 years, and it is male-predominant. The prevalence of BrS is estimated to be 1–5 per 10,000 people in Caucasians but is higher in Southeast Asians (12 per 10,000). Over 25 years, the pathophysiologic mechanism of BrS still remains elusive because of limited genetic information. *SCN5A* is the major BrS-causing gene responsible for approximately 20% of BrS cases in Caucasians and 7.5–8% of cases in Han Chinese. Although several susceptibility genes have been identified, a genetic cause remain unknown in approximately 80% of BrS patients. Copy number variants (CNVs) can contribute to disease susceptibility, but their role in Brugada syndrome (BrS) is unknown.

Added value of this study

In this study, we enrolled 335 unrelated BrS patients from 2000 to 2018 in the Taiwanese population using a 2-stage approach with extreme phenotype sampling strategy. We used microarray and exome sequencing for discovery phase whereas Sanger sequencing were used for validation phase. We performed patch clamp study using HEK293 cells and *gstm3* knockout zebrafish experiments to characterize the CNV function. We identified a diallelic deletion of *GSTM3* contains the eighth exon and the transcription stop codon, and functional studies showed that this *GSTM3* deletion is associated with reduced cardiac sodium channel current. In this Taiwanese BrS patient cohort, the frequency of a copy number deletion of *GSTM3* was observed in 23.9% of 301 BrS patients without *SCN5A* mutations versus 0.8% of 15,829 ancestry-matched healthy controls in Taiwan Biobank. Intriguingly, the *GSTM3* deletion is not reported in the large dataset based on whole-genome sequences (>10,000 individuals), suggesting that it is closely associated with BrS. We also found that BrS patients carrying the *GSTM3* deletion had higher rates of sudden cardiac arrest and syncope compared to those without.

Implications of all the available evidence

We propose that our finding have both diagnostic and risk stratification clinical impacts for patients with BrS. Our study identified a deletion of *GSTM3* in BrS patients, which is associated with reduced I_{Na} , suggesting that the deletion could be a genetic modifier of the BrS phenotype. This study drives the understanding of this disease forward. This variant may be a novel genetic modifier/risk predictor for the development of the electrocardiographic and arrhythmic manifestations of BrS. It could be used as a risk predictor in patients with BrS for clinical practice. The gene could also be a potentially future therapeutic target and clinical genetic testing for patient care.

remains unknown in approximately 80% of BrS patients. One primary reason for this lack of causal certainty is the fact that a large proportion of patients is likely to represent non-Mendelian cases with oligogenic inheritance [8]; phenotyping errors, inadequate sensitivity of screening methods, and mutations in non-coding regions or in unknown genes are additional sources of causal uncertainty. Another possibility may be the presence of copy number variations (CNVs) in genes affecting the onset of BrS, which are known to play a role in cardiovascular diseases [9,10]. However, there is limited evidence regarding whether CNVs are important in BrS.

Here, we conducted a genome-wide CNV study in BrS patients without *SCN5A* mutations using a multi-stage study design with extreme phenotype sampling strategy [11,12]. We initially used genome-wide microarray to screen CNV regions in a case-control design, then used whole exome sequencing (WES) to fine-tune the length of candidate CNV regions in BrS patients because the candidate CNV regions were too long for Sanger sequencing technology. Thereafter, we validated the candidate CNV region in an independent BrS patient cohort using Sanger sequencing. We compared the frequency of identified CNV regions in the healthy populations using in-house controls from Taiwanese, the Taiwan Biobank (TWB), and the genome aggregation database (gnomAD). Finally, we used cell and zebrafish models to investigate the functional role of the identified CNVs in BrS patients.

2. Materials and methods

2.1. Study subjects

We consecutively recruited 335 unrelated patients with BrS from 2000 to 2018 in the Taiwanese population in Taiwan; 76 were identified via symptoms of sudden cardiac arrest (SCA) or syncope early in the study period (2000–2010) and 259 more, both symptomatic and asymptomatic, were identified later (2011–2018), after the SADS-TW BrS registry increased awareness of BrS [13]. Aborigines were excluded from this study. BrS was diagnosed by 2 independent cardiologists using established criteria (Shanghai BrS Score ≥ 3.5) [14]. Since *SCN5A* is the major BrS-causal gene [4], we screened it first. Peripheral blood samples were collected from all participants. Mutations or SNPs in the *SCN5A* gene were screened using direct sequencing. We followed the primers and PCR conditions published by Wang et al. [15] to perform genotyping in all amino acid-coding exons and intron borders of *SCN5A*. Amplicons were purified by solid-phase extraction and were bidirectionally sequenced using a PE Biosystems Taq DyeDeoxy terminator cycle sequencing kit (PE Biosystems, Foster City, CA, USA). Sequencing reactions were separated on a PE Biosystems 373A/3100 sequencer, and the results were compared with a reference sequence from GenBank and the TWB. The pathogenicity of a mutation was defined by American College of Medical Genetics and Genomics guidelines [16]. Exclusion of 34 BrS patients with *SCN5A* mutations left 301 unrelated BrS patients enrolled in this CNV study.

The prevalence of BrS is lower (0.05–0.1%) [1,17] than that of common diseases (e.g., hypertension (28–31%) [18]). To overcome the small case number, we used a 2-stage study design with extreme phenotype sampling strategy and 2 independent cohorts with increasing sample size which attempted to maximize power and efficiency [11,12] (Fig. 1). In stage I, we initially selected 66 BrS patients (cohort 1, discovery cohort) to discover candidate CNV regions by microarray and WES. In stage II, cohort 2 (replication cohort, 235 unrelated BrS) were used to confirm the significant CNVs using PCR-based genotyping assay and Sanger sequencing. This study was approved by the ethics committee of National Taiwan University Hospital. All participants gave informed consent before participating in the study.

Southeast Asians (12 per 10,000) [1,2]. The average age at diagnosis is 40 ± 22 years, and it is male-predominant [3].

SCN5A, which encodes the cardiac sodium channel, is the major BrS-causing gene responsible for approximately 20% of BrS cases in Caucasians and 7.5–8% of cases in Han Chinese [4,5]. Although several susceptibility genes have been identified [1,6,7], a genetic cause

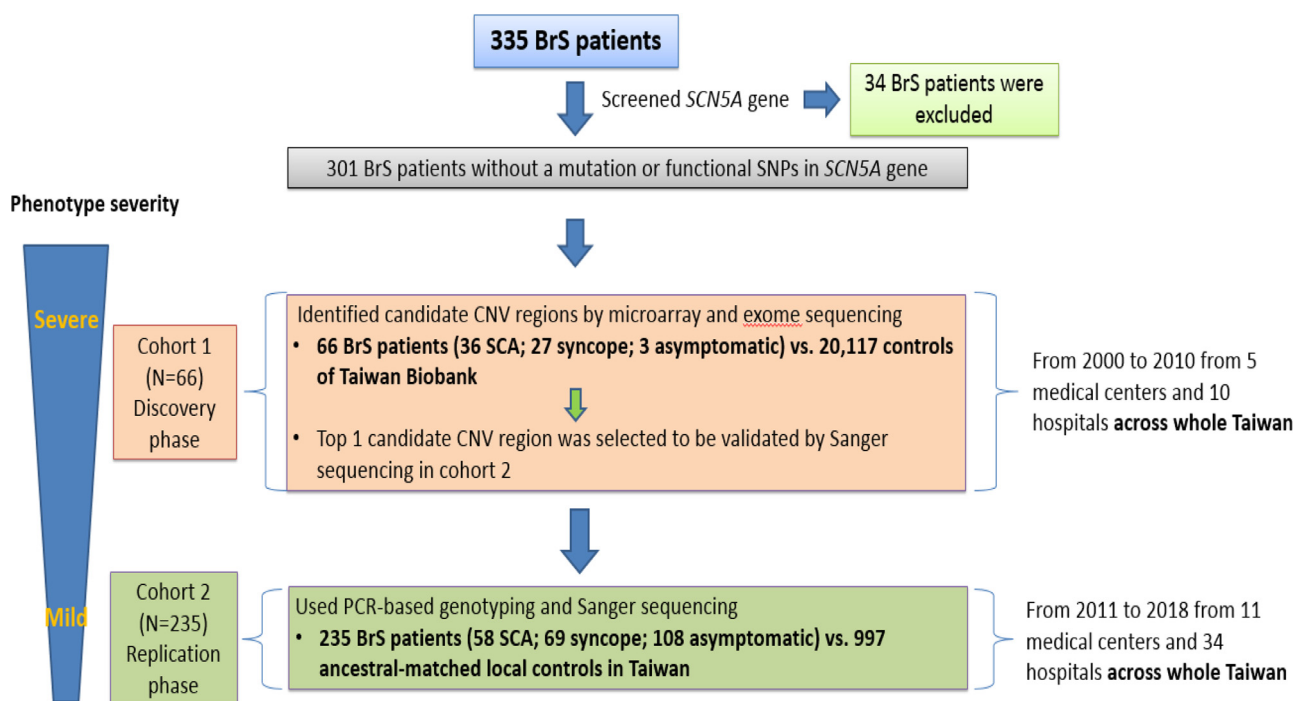


Fig. 1. An illustration of the timeline and experimental workflow of this study. This study used 2-stage design with extreme phenotype sampling strategy with two independent BrS cohorts.

2.2. Microarray experiments, exome sequencing and CNV analysis

Omni1-Quad BeadChip microarrays (Illumina, USA) were performed according to the manufacturer's instructions. The data were submitted to the Gene Expression Omnibus (accession number GSE46348). To evaluate whole-genome CNV regions, raw intensity data from 1.14 million SNPs and CNV probes were imported into Partek Genomics Suite software (Partek Inc., USA) to perform CNV analysis. The criteria used for identifying CNV regions are shown in the Supplementary Note and the accuracy of the segmentation algorithm has been discussed in a previous study [19]. Lastly, Ingenuity Pathway Analysis (Ingenuity Systems, Inc., USA) was performed to characterize the biological functions of genes located in CNV regions. We used WES to fine-tune the length of candidate CNV regions. The detailed procedures of WES are described in the Supplementary Note. The CNVkit (v0.9.4) algorithm was used to obtain genome-wide CNV regions of each sample while the flat reference was set as the identical coverage in all samples [20]. A CNV region was defined as a deletion if its copy number was less than 1.2.

2.3. Validation of identified CNV regions

To further minimize the chance that false associations arose as a result of technical genotyping artefacts [21], different platforms using PCR-based genotyping and Sanger sequencing were used to validate the results of microarray and WES. To confirm the region containing the deletion of *GSTM3* identified by genome-wide microarray and WES, we designed PCR primers for the region with the lowest copy number of *GSTM3*. Forward and reverse primers used to amplify target regions are listed in **Table S1**, and the detailed procedures are given in the Supplementary Note.

2.4. Investigation of the identified CNV region in local controls and a public control

To evaluate the CNV frequency of *GSTM3* in relatively healthy populations, we used 2 local controls and 1 public control. For the

first local controls, we first performed PCR and Sanger sequencing in 997 ancestral-matched in-house controls. In-house controls were ancestral-matched individuals with no arrhythmia-related symptoms, normal coronary arteries by angiography, normal 12-lead electrocardiogram (ECG), and no family history of sudden cardiac death (SCD), BrS, or heart failure. For the second local controls, we analysed genotyping data from the TWB (20,117 participants; <https://taiwanview.twbiobank.org.tw/search>, Supplementary Note). The design of the TWB array was a joint effort of the TWB, the National Center of Genome Medicine (NCGM; http://ncgm.sinica.edu.tw/ncgm_02/index.html), and Affymetrix, Inc. To compare with other ethnicities, we used the gnomAD structural variants (SVs) database to examine the *GSTM3* deletion frequency in major worldwide populations.

2.5. Basal expression of *GSTM3* gene in human adult right ventricle

BrS is believed to be a right heart disease [22]. Although *GSTM3* is expressed in human heart muscle [23], whether *GSTM3* is specifically expressed in right ventricular cells has never been investigated before. We used a cDNA library from a healthy human adult right ventricle (Invitrogen) and diluted it to a working concentration of 100 ng/ μ L. Then, using primers for human β -actin (*ACTB* gene) and *GSTM3*, we performed PCR and separated the products on a 2% agarose gel to check the amplified band.

2.6. Western blot of *GSTM3* proteins extracted from HEK293 cells and HL-1 cells

HEK293 cells (derived from human embryonic kidney) were grown in Dulbecco's modified Eagle medium (DMEM) supplemented with 10% fetal bovine serum (FBS), L-glutamine, and penicillin/streptomycin at 37 °C, 5% CO₂. HL-1 cardiac muscle cells, an immortalised mouse atrial cell line, were cultured on a plate coated with gelatin/fibronectin, maintained in Claycomb medium containing 10% FBS, penicillin/streptomycin, L-glutamine, and 0.1 mM norepinephrine. Protein lysates (50 μ g) were extracted from HEK293 cells, HL-1 cells, and mouse testis tissue (use as positive control), then separated by

SDS-PAGE, blotted with the *GSTM3* antibody (Cusabio Technology, LLC), and detected using an enhanced chemiluminescence western blotting system (Amersham Biosciences). *GSTM3* protein is endogenously expressed in HEK293 cells but not in HL-1 cells (Fig. S1). Therefore, we used HEK293 cells stably expressing Nav1.5 channel in further studies.

2.7. HEK293 cell culture and transfection

HEK293 cells stably express *SCN5A* (encoding the Nav1.5 channel), hereafter referred to as HEK Nav1.5 cells. HEK Nav1.5 cells were cultured in a controlled environment (5% CO₂, 37 °C) and maintained in DMEM (Euroclone, Italy) supplemented with FBS (10%), L-glutamine (2 mM), penicillin/streptomycin (100 U/mL, 100 µg/mL), and zeocin (200 µg/mL). The transfection was carried out using jetPRIME reagent (PolyPlus transfection, Illkirch, France) according to the manufacturer's instructions. Cells were transfected with *GSTM3* Silencer Select Pre-designed siRNA (20 nM; Ambion, Thermo Fisher Scientific, Italy) or with Silencer Select Negative Control #1 Pre-designed siRNA, a non-targeting siRNA providing a negative control to compare siRNA-treated samples (20 nM; Ambion, Thermo Fisher Scientific, Italy). Twenty-four hours after transfection, cells were harvested either to analyze the knockdown of endogenous *GSTM3* protein levels by western blotting or for cytotoxicity assays, or re-seeded for electrophysiological recording.

2.8. Western blot of *GSTM3* protein extracted from HEK NAV1.5 cells transfected with siRNA specific for *GSTM3* or with a non-targeting negative control siRNA

Cells were lysed and cytoplasmic proteins were extracted using a NE-PER® Nuclear and Cytoplasmic Extraction Reagents kit (Thermo Fisher Scientific, Italy). Protein concentrations were determined using Bradford assay reagent (Pierce Coomassie Plus Protein Assay; Thermo Fisher Scientific, Italy) following the manufacturer's instructions. Twenty-five µg of cytoplasmic protein were separated on homemade gels (12% acrylamide) in a standard running buffer and then transferred onto nitrocellulose membranes (GE Healthcare, Euroclone, Italy). Membranes were blocked with 5% non-fat dry milk in 1 × Tris-buffered saline containing 0.1% Tween 20 (TTBS 0.1%) for 90 min at room temperature, washed 3 times in TTBS 0.1%, and then incubated overnight at 4 °C with anti-α-tubulin (1:500 in TTBS 0.1% plus milk 5%, rabbit monoclonal; Cell Signaling, Danvers, MA, USA) and anti-human glutathione S-transferase mu 3 (1:1000 in TTBS 0.1% plus milk 5%, rabbit polyclonal; Cusabio Biotech Co, College Park, MD, USA). After 3 TTBS 0.1% washings, membranes were incubated for 90 min with an IgG HRP-conjugated antibody (donkey anti-rabbit, 1:5000 in TTBS 0.1% plus milk 1%; Santa Cruz Biotechnology) and then washed again 3 times in TTBS 0.1%.

Proteins were detected using an enhanced chemiluminescence detection kit (SuperSignal West Pico Chemiluminescent Substrate; Thermo Fisher Scientific, Italy) in an ImageQuant LAS 4000 instrument (GE Healthcare Life Sciences, Italy). Blots were analysed and quantified with ImageJ software.

2.9. Cytotoxicity assays

To measure the mitochondrial activity and membrane damage in HEK293 cells, 3-(4,5-dimethylthiazol-2-yl)-2,5-diphenyltetrazolium bromide (MTT) (MTT Formazan powder; Sigma-Aldrich, Italy) and lactate dehydrogenase (LDH) (LDH Cytotoxicity Detection KitPLUS; Sigma-Aldrich, Italy) assays were performed following the manufacturer's instructions as in our previous work [24]. To create conditions of oxidative stress, cells were incubated for 30 or 60 min either with medium or with medium plus 15 mM tert-butyl hydroperoxide (tBHP; Sigma-Aldrich, Italy). Absorbance and emission were

measured with a multi-label spectrophotometer (VICTOR3, Perkin Elmer, USA) at 570 nm and 490 nm, respectively.

2.10. Electrophysiological experiments in HEK NAV1.5 cells

Patch clamp experiments were performed at room temperature in HEK Nav1.5 cells in whole cell configuration. The experimental details are described in the Supplementary Note. To induce conditions of oxidative stress, cells were incubated for 30 min at room temperature with an extracellular solution containing 95 mM N-methyl-D-glucamine, 20 mM NaCl, 5 mM CsCl, 2 mM CaCl₂, 1.2 mM MgCl₂, 10 mM HEPES, 5 mM glucose, and 15 mM tBHP, and recordings were obtained within 60 min from the beginning of treatment. The standard voltage clamp protocols have been previously described [25,26]. Membrane voltages were not corrected for liquid junction potential. To measure the kinetics of the onset of inactivation, the declining phase of I_{Na} traces recorded between -30 mV and 20 mV were fitted with a bi-exponential function. The number of cells is indicated in Table 3, and the "current density" column is greater than the "activation" column because not all cells could complete the protocol for the study of the activation properties. We did not consider applying TTX in order to define I_{Na}, as HEK Nav1.5 cells stably express Nav1.5 channel, and the comparison with the un-transfected HEK293 cells showed the absence of inward currents (Fig. S2).

2.11. Generation and characterization of CRISPR/Cas9-mediated *GSTM3* knockout male adult zebrafish

All experimental procedures on zebrafish were approved by the committee for use of laboratory animals at National Taiwan University, Taipei, Taiwan (IACUC Approval ID: 103; Animal Use document no. 102) and carried out in accordance with the guidelines of the Animal Welfare Act. The details of generation and characterization of *GSTM3* knockout adult male zebrafish using CRISPR/Cas9 are described in the Supplementary Note. Briefly, among the 3 guide RNAs (gRNAs) tested, only the exon 5-targeted gRNA effectively induced distinct changes in melting curves compared to the untreated groups (Fig. S3A). We thus raised only the exon 5 gRNA-treated F0 embryos to adulthood and then crossed them with WT fish to obtain F1 embryos. The F1 embryos were raised to 2 months old to collect genomic DNA from their tail fins. We screened for the *GSTM3* mutation carriers by high resolution melting analysis, raised them to adulthood, and cross-bred them to obtain the F2 generation. The zygosity of the F2 fish was determined by capillary electrophoresis. We performed PCR using F2 fish tail fin genomic DNA to obtain amplicons from 24 fish. As shown in Fig. S3B, the WT fish showed only one band of 250 base pairs. In contrast, the homozygous mutant fish also had one band with a reduced size, which indicated a potential deletion in the *GSTM3* gene. The heterozygous fish contained both bands with reduced intensity. To confirm the deletion in *GSTM3*, we sequenced those amplicons and found that all *GSTM3*^{-/-} fish had a 7 bp deletion (-TCCGCAA-) at the gRNA binding site compared to the sequence of WT fish (Fig. S3C).

The WT *GSTM3* protein contains 219 amino acids. The deletion results in a premature stop codon in the middle. The mutant *GSTM3* has the native sequence of 106 amino acids at its N-terminus, followed by 25 mutated amino acids due to the frameshift. The amino acid sequence alignment of WT and mutant *GSTM3* is presented in Fig. S4. The identified *GSTM3*^{+/-} and *GSTM3*^{-/-} fish were separated and used for further experiments.

2.12. Expression of *GSTM3* in adult male zebrafish heart by real-time quantitative PCR

To examine expression of *GSTM3*, we isolated 3 hearts of adult male zebrafish. The hearts were homogenised to extract total RNA

using TRIzol reagent (Invitrogen) for cDNA synthesis using the High-Capacity cDNA Reverse Transcription kit (Applied Biosystems) according to the manufacturer's instructions. The cDNA was then subjected to real-time quantitative PCR analysis (Applied Biosystems). Taqman reactions were performed using one-step RT-PCR Master Mix Reagents with the ABI PRISM 7700 Sequence Detection System and analysed using the Sequence Detection System software. Gene expression was normalised to a commonly used reference gene (*EF1A*, elongation factor 1 α). Primers and probes were based on GenBank sequences (*GSTM3*, NM_001162851.1; and *EF1A*, NM131263.1). The data were analysed using the relative gene expression (i.e., $\Delta\Delta CT$) method, as described in Applied Biosystems User Bulletin No. 2 and explained further by Livak and Schmittgen [27]. Briefly, the data were presented as the fold change in gene expression normalised to *EF1A* and relative to a calibrator. The results are presented in Fig. S5.

2.13. Arrhythmogenicity assessment and drug administration in zebrafish

Because BrS is a young adult male-dominant disease, we used adult male zebrafish (F2) for further experiments instead of larva. All experiments were performed at room temperature. The PR interval, RR interval, QT interval, and QRS duration were recorded. The PR interval was measured from the start of the P wave to the start of QRS. The QT interval was defined as the time from the start of the Q wave to the end of the T wave. QRS duration was defined from the start of the Q wave to the end of the S wave. The heart rate was measured from the RR interval, defined as the time interval between the peaks of 2 consecutive QRS complexes. Recordings were acceptable if the T-wave amplitude was $\geq 25 \mu V$ and did not deteriorate by $\geq 50\%$ during the recording. Bazett's formula was used to correct the observed QT interval for variations in heart rate.

Since sodium channel blockers are known to unmask Brugada ECG in patients and induce arrhythmia [4], we performed a flecainide challenge in the *GSTM3*^{-/-} adult zebrafish [28]. Because quinidine is used clinically to suppress the electrocardiographic and arrhythmic manifestations of BrS [4], we tested its ability to suppress arrhythmias in a zebrafish model of BrS. Drugs were diluted from DMSO stock solutions to final concentrations of 0.1 μM , 1 μM , or 10 μM in E3 solution. All concentrations were safe for adult zebrafish [29,30].

Wild-type (WT) and mutant 9–12 month-old adult male zebrafish (F2) were anaesthetised by titration with tricaine solution (MS-222, Sigma) for 2 min. We administered flecainide and quinidine. Arrhythmias, PR interval, RR interval, QRS duration, QT interval, and QTc values were obtained at baseline and after 10 min of exposure to drug (Fig. S6). All parameters were recorded for 10 min after reaching a stable steady state. We performed programmed extra-systolic stimulation (PES) before and after drug administration as a previously study [31]. Two independent and blinded investigators confirmed all measurements. The Inter-observer agreement was determined by overall proportion of agreements and by using the Kappa statistic. The overall proportion of agreement in the ECG measurements among the two interpreters was 99.7% with a Kappa score of 0.95. If the ECG data had a discrepancy, we discarded the data. The details of the procedure and the PES protocol are described in the Supplemental Note.

2.14. Statistical analyses

Continuous variables were compared using the Student's *t*-test. Categorical variables and CNV proportions were analysed using the Fisher's exact test. The analysis of variance (ANOVA) method was performed for multiple group comparisons, followed by a modified *t*-test with Fisher LSD correction (ORIGIN 10). *P* values <0.05 were considered as statistically significant.

3. Results

3.1. Patient characteristics

The demographic characteristics of the study cohorts are shown in Table 1. The gender of all cohorts was male-predominant, and 63.1% of BrS patients overall were symptomatic. As expected, the percentage of the symptomatic BrS patients was higher in cohort 1 than in cohort 2 (95.5% vs. 54%), whereas the percentage of asymptomatic BrS patients was higher in cohort 2 than in cohort 1 (4.5% vs. 46%) because of our study design. There were no differences in gender, family history of SCD, and spontaneous type 1 Brugada ECG among the 2 cohorts.

3.2. Discovery of the CNV regions

The genomic landscape of CNV regions in BrS patients is illustrated in Fig. S7. A total of 502 aberrant regions were observed, including 447 deletions and 55 amplifications. Importantly, no CNVs were detected in the *SCN5A* gene. The Refseq database revealed 91 deleted and 11 amplified genes in total (Table S2). Among these 102 CNV genes, Ingenuity Pathway Analysis revealed 5 significantly enriched canonical pathways ($P < 10^{-5}$, Table S3, Hypergeometric test). Notably, although the 5 pathways had different cellular functions, they were primarily identified on the basis of the same genes, particularly the GST mu family. Unexpectedly, all 5 genes in the GST mu family, including *GSTM1*-5, showed high frequencies of deletion, suggesting they make up a gene cluster deleted in BrS. Among the 5 genes, *GSTM3* is the gene nearest to the breakpoint of the CNV region spanning across the GST mu family. Therefore, *GSTM3* was selected for further investigations. Because the candidate CNV region of *GSTM3* (chr1:109,733,932-109,739,407) was too long (>5 K bp) to use traditional Sanger sequencing to identify the breakpoints of this CNV region, we used WES technology to fine-tune this candidate CNV region in the unrelated 66 BrS patients instead. Fifteen of the 66 BrS patients (30%) had this *GSTM3* deletion, and WES showed the length of the *GSTM3* deletion (chr1:109,737,076-109,737,247, hg38) (Fig. 2A). Except for common variants (e.g., SNPs), no radical or mis-sense mutations were identified in the *GSTM3* gene.

3.3. Validation and replication

In cohort 2, the *GSTM3* deletion was present in 23.4% of the 235 BrS patients using a PCR-based genotyping assay and direct sequencing (Fig. 2B and 2C). The length of the *GSTM3* deletion is 291 base-pairs (chr1:109,737,011-109,737,301, hg38). Importantly, this deletion region in *GSTM3* contains exon 8 and the transcription stop codon (CCDS 812.1, hg38). In total, 23.9% of the BrS patients carried the *GSTM3* deletion and 94.4% of the BrS patients with the *GSTM3* deletion (68/72) were heterozygous carriers. Interestingly, when we screened this CNV in the 34 BrS patients excluded for having *SCN5A*

Table 1
Clinical characteristics of BrS patients in 2 independent cohorts.

	Cohort 1 (N = 66)	Cohort 2 (N = 235)	All (N = 301)
Age at diagnosis (years)	42.0 \pm 12.9	45.0 \pm 15.8	44.3 \pm 15.2
Gender (male)	63 (95.4%)	209 (88.9%)	272 (90.4%)
Presentations			
SCA	36 (54.5%)	58 (24.7%)	94 (31.2%)
Syncope	27 (40.9%)	69 (29.4%)	96 (31.9%)
No symptoms	3 (4.5%)	108 (46.0%)	111 (36.9%)
Family history of SCD	13 (19.7%)	49 (20.9%)	62 (20.6%)
Spontaneous type 1 Brugada ECG	59 (89.4%)	176 (74.9%)	235 (78.1%)

BrS, Brugada syndrome; ECG: electrocardiogram; SCD: sudden cardiac arrest.

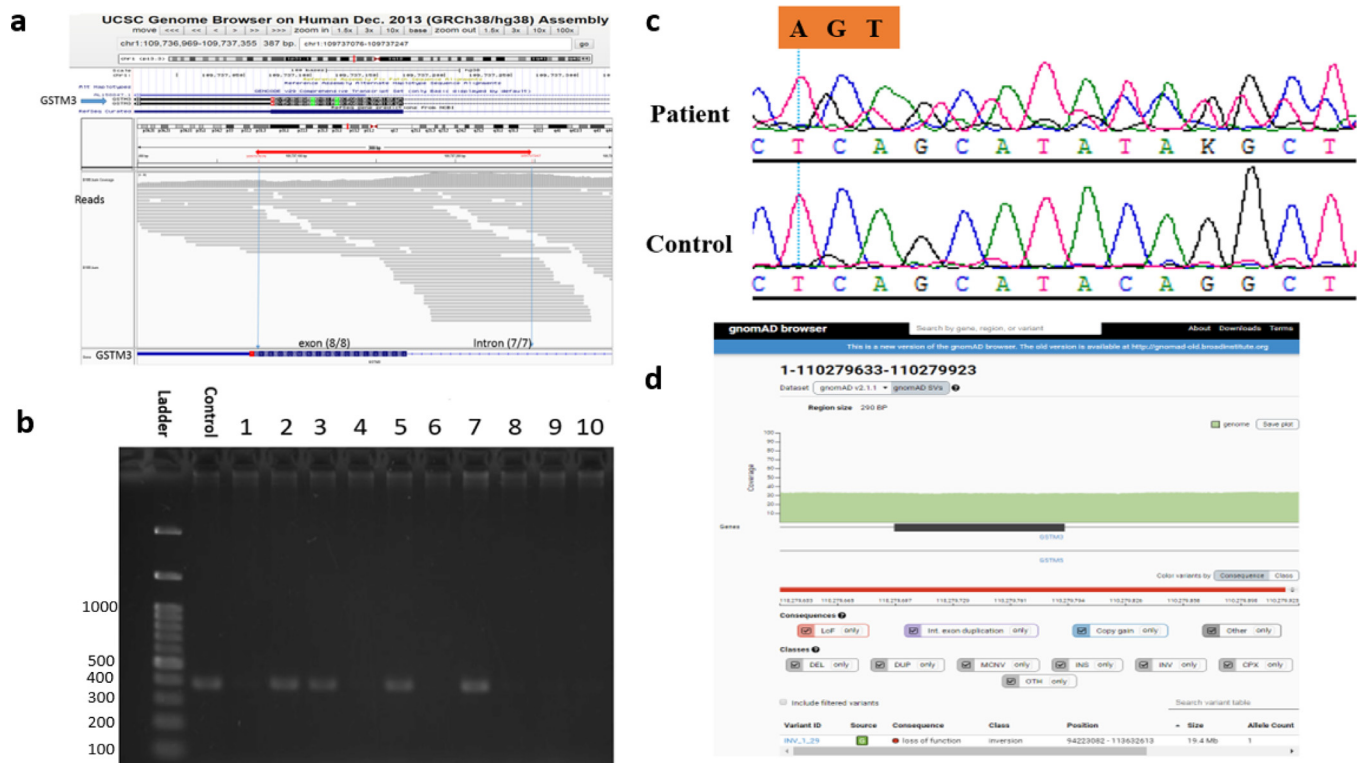


Fig. 2. Validation of the *GSTM3* deletion. (A) An example of a plot of *GSTM3* deletion detected by WES in a BrS patient. Red labels indicate the chromosomal position (chr1:109,737,076-109,737,247, hg38), containing part of intron 7, part of exon 8, and the transcription stop site (CCDS 812.1, hg38). (B) An example of a polyacrylamide gel of *GSTM3*. A PCR band indicated no deletion or heterozygous deletion of *GSTM3* (copy number=1 or 2; patients 2, 3, 5, 7 and control); no PCR band indicated homozygous deletion of *GSTM3* (copy number=0; patients 1, 4, 6, 8, 9 and 10). (C) An example of the sequencing map of part of the deletion in exon 8 of *GSTM3* containing the transcription stop codon by a reverse primer in a BrS patient with heterozygous deletion and a control without deletion. (D) No *GSTM3* deletion (chr1:110,279,633-110,279,923, hg37) is reported in the gnomAD structural variants database ($N = 10,738$ unrelated individuals, (https://gnomad.broadinstitute.org/region/1-110279562-110279935?dataset=gnomad_sv_r2)).

mutations, this CNV was not detected. Co-segregation analysis in 10 families showed that the co-segregation rate was 20% (2 of 10 families; **Fig. S8, Supplementary Note**).

3.4. Evaluation of the *GSTM3* deletion in the healthy controls

We evaluated the frequency of the *GSTM* deletion in 3 healthy controls (2 ancestral-matched local controls and 1 public CNV database). In the 2 local controls, the deletion was in 0.1% of 997 in-house unrelated controls whereas CNV analysis showed that 0.8% of the 15,829 ancestral-matched unrelated samples which passed the quality assessment have the *GSTM3* deletion in the TWB, which were significantly lower than that in BrS patients (both $P < 0.001$, Proportional test). In the public CNV database, the WGS data from the gnomAD SVs database, which is 9% East Asian, showed that no such deletion in *GSTM3* was reported in any samples out of 10,738 unrelated individuals ($P < 0.0001$, **Fig. 2D**, Proportional test). These results support the deletion of *GSTM3* being significantly associated with Taiwanese BrS patients without *SCN5A* mutations.

3.5. Comparison of clinical demographics and severity of clinical presentation of the BrS patients with and without the deletion of *GSTM3*

The comparison of clinical characteristics between BrS patients with or without this deletion is shown in **Table 2**. In cohort 1 and cohort 2, there were no significant differences in age at diagnosis, gender, family history of SCD, or spontaneous type 1 Brugada ECG between the two cohorts. In cohort 1 and cohort 2, a higher percentage of BrS patients with deletion of *GSTM3* experienced SCA compared to those without ($P = 0.003$, 0.007 , respectively, Fisher's exact

test). In total cohort, more BrS patients with deletion of *GSTM3* experienced SCA and syncope than those without ($P = 0.002$, 0.04 , respectively, Fisher's exact test).

3.6. Establishment and validation of the cellular model

After confirming that *GSTM3* is expressed in human adult right ventricle (**Fig. S9**), we established a cellular model consisting of HEK293 cells stably expressing the *SCN5A* (HEK Nav1.5). To mimic the *GSTM3* deletion observed in BrS patients, we induced the down-regulation of *GSTM3* expression by transfecting the cells with siRNA targeting *GSTM3*. Western blotting showed that siRNA transfection reduced *GSTM3* expression by almost 50% (**Fig. 3A**).

To test the effects of *GSTM3* silencing on cell vitality, we used tBHP (15 mM), an organic peroxide, to create conditions of oxidative stress [32,33]. MTT assays showed that mitochondrial activity was reduced equally after 60 min of tBHP exposure in the negative control ($84.4 \pm 11.5\%$ vitality, $P = 0.015$, ANOVA, followed by a modified t-test with Fisher LSD correction) and in the *GSTM3*-silenced cells ($87.5 \pm 8.7\%$ vitality, $P = 0.028$, ANOVA, followed by a modified t-test with Fisher LSD correction) (**Fig. 3B**). LDH activity in the culture medium was also measured as an index of membrane damage after tBHP exposure. Again, the effect of tBHP on cell vitality was indistinguishable in control and *GSTM3* siRNA-transfected cells ($81.8 \pm 1.8\%$ vitality, $P = 1.04 \times 10^{-4}$; and $83.3 \pm 1.8\%$ vitality, $P = 9.6 \times 10^{-6}$, respectively, ANOVA, followed by a modified t-test with Fisher LSD correction) (**Fig. 3C**). These data suggested that tBHP-induced cytotoxicity under these conditions was not critically relevant, at least from the metabolic point of view.

Table 2
Comparisons of clinical characteristics between BrS patients with or without deletion of *GSTM3*.

	Cohort 1 (discovery cohort)			Cohort 2 (replication cohort)			All		
	With the CNV deletion of <i>GSTM3</i> (N = 25)	Without the CNV deletion of <i>GSTM3</i> (N = 41)	OR (95% CI)	With the CNV deletion of <i>GSTM3</i> (N = 47)	Without the CNV deletion of <i>GSTM3</i> (N = 188)	OR (95% CI)	With the CNV deletion of <i>GSTM3</i> (N = 72)	Without the CNV deletion of <i>GSTM3</i> (N = 229)	P value
Age at diagnosis (years)	42.9 ± 11	41.5 ± 14	0.67	45.5 ± 15	44.9 ± 16	0.81	44.6 ± 13.7	44.3 ± 15.7	0.88
Gender (male)	24 (96.0%)	39 (95.1%)	1	43 (91.5%)	166 (88.3%)	0.79	67 (93.1%)	205 (89.5%)	0.49
Presentations									
SCA	18 (72.0%)	18 (43.9%)	0.04*	19 (40.4%)	39 (20.7%)	0.007*	37 (51.4%)	57 (24.9%)	<0.001*
Syncope	7 (28.0%)	20 (48.8%)	0.41 (0.12–1.32)	23 (48.9%)	46 (24.5%)	2.94 (1.44–6.03)	30 (41.7%)	66 (28.8%)	1.76 (1.02–3.05) 0.04*
No symptoms	0 (0%)	3 (7.3%)	0.28	5 (10.6%)	103 (54.8%)	0.10 (0.03–0.27)	5 (6.9%)	106 (46.3%)	0.09 (0.03–0.23) <0.001*
Family history of SCD	7 (28.0%)	6 (14.6%)	2.24 (0.55–9.42)	11 (23.4%)	38 (20.2%)	1.21 (0.51–2.70)	18 (25.0%)	44 (19.2%)	1.40 (0.71–2.72) 0.32
Spontaneous type 1 Brugada ECG	23 (92.0%)	36 (87.8%)	1.59 (0.23–17.97)	0.7	39 (83.0%)	1.81 (0.77–4.79)	62 (86.1%)	174 (76.0%)	1.96 (0.91–4.57) 0.07
Fragmented QRS	2	2	1.68 (0.11–24.67)	0.63	3	1.53 (0.25–6.72)	5	10	1.63 (0.42–5.46) 0.36
PR interval in V1 (ms)	168±23	167±15	0.83	173 ± 30	170 ± 31	0.55	171±28	169±29	0.60
QRS duration in V1 (ms)	110±22	102±15	0.08	109±21	106±17	0.09	109.3 ± 21.2	105.3 ± 16.7	0.10
QTc in V1 (ms)	416±47	407±26	0.31	438±51	430±38	0.23	430±50	426±37	0.47
Tpeak-Tend interval in V1 (ms)	92±18	82±13	0.01	88±17	83±12	0.02	89.4 ± 17.3	82.8 ± 12.1	<0.001*
QT/QRS duration in V1	3.9 ± 1.1	3.7 ± 0.8	0.40	4 ± 0.9	3.8 ± 0.7	0.10	3.97±0.98	3.78±0.72	0.08

BrS: Brugada syndrome; ECG: electrocardiogram; SCA: sudden cardiac arrest; SCD: sudden cardiac death; *P < 0.05 by Fisher's exact test or Student's t-test.

3.7. Effect of the loss of *GSTM3* on the cardiac sodium current under conditions of oxidative stress

Whole-cell patch-clamp data showed that Nav1.5 current density measured at -10 mV was not affected by the siRNA transfections (Fig. 4A-B; Table 3). As expected from the literature [32,33], a condition of oxidative stress, created by the application of 15 mM of tBHP, triggered a decrease in I_{Na} of about 60% both in control cells and in cells transfected with the siRNA negative control. However, when *GSTM3* protein expression was silenced, tBHP reduced the I_{Na} density by approximately 75% (Fig. 4A-B; Table 3) and the onset of fast inactivation was accelerated (Fig. 3C).

Consistent with previous studies [34,35], no significant differences were found in activation after tBHP application (Fig. 5; Table 3), but tBHP exposure induced a significant negative shift in the availability of sodium channels (Fig. 5). When HEK Nav1.5 cells were treated with tBHP, $V_{1/2}$ significantly shifted approximately 8 mV in the negative direction, and a similar shift was observed in cells transfected with the non-targeting siRNA (Table 3). This hyperpolarizing shift was even more dramatic (approx. -18 mV) when *GSTM3* expression was reduced, after induction of oxidative stress (Fig. 5; Table 3). These data support the hypothesis that reduced expression of *GSTM3* amplifies the response of Nav1.5 channels to oxidative stress, causing a more dramatic reduction in I_{Na} .

3.8. Comparisons of baseline ECG parameters and ventricular arrhythmic events before and after flecainide administration

Table S4 shows the ECG parameters and the number of WT, *GSTM3*+/- and *GSTM3*-/- zebrafish with ventricular arrhythmia (VA) before and after flecainide administration. The baseline PR interval, QRS duration, RR interval, and QTc interval were not significantly different among the 3 groups. After flecainide treatment (1 μM and 10 μM flecainide), there was a significant increase of PR interval and QRS duration in *GSTM3*+/- and *GSTM3*-/- zebrafish compared with WT. At baseline, the number of WT, *GSTM3*+/-, and *GSTM3*-/- zebrafish with VA was not different but the number of *GSTM3*+/- and *GSTM3*-/- zebrafish with VA significantly increased after flecainide administration (Fig. 6A-C). Interestingly, the number of *GSTM3*+/- and *GSTM3*-/- zebrafish with VA decreased after quinidine infusion (Fig. 6D-F, Table S5). The pharmacologic responses observed in *GSTM3*-/- and *GSTM3*+/- fish are congruent with those encountered in clinical cases of BrS.

3.9. Comparison of arrhythmogenicity after programmed extra-systolic stimulation

Table S5 shows the number of WT, *GSTM3*+/- and *GSTM3*-/- zebrafish with inducible ventricular tachycardia (VT) or ventricular fibrillation (VF) after PES. After PES in the absence of drug treatment, the number of *GSTM3*+/- and *GSTM3*-/- zebrafish with inducible VT or VF was significantly higher than WT fish. With flecainide administration, the number of *GSTM3*+/- and *GSTM3*-/- zebrafish with inducible VT or VF increased significantly. In contrast, the number of zebrafish with inducible VT or VF among the 3 groups was not different after quinidine infusion except for 0.1 μM quinidine.

4. Discussion

Previous CNV studies in BrS focused on the *SCN5A* gene alone [36-40]. This is the first whole-genome CNV study to investigate the role of genomic CNVs in influencing susceptibility to BrS and to examine the role of CNV in risk stratification of BrS patients. We identified a diallelic CNV deletion of *GSTM3* in 23.9% of Taiwanese BrS patients without *SCN5A* mutations. In contrast, the deletion of *GSTM3* was rarely observed in 0.1% of in-house controls (N = 997) and 0.8% in

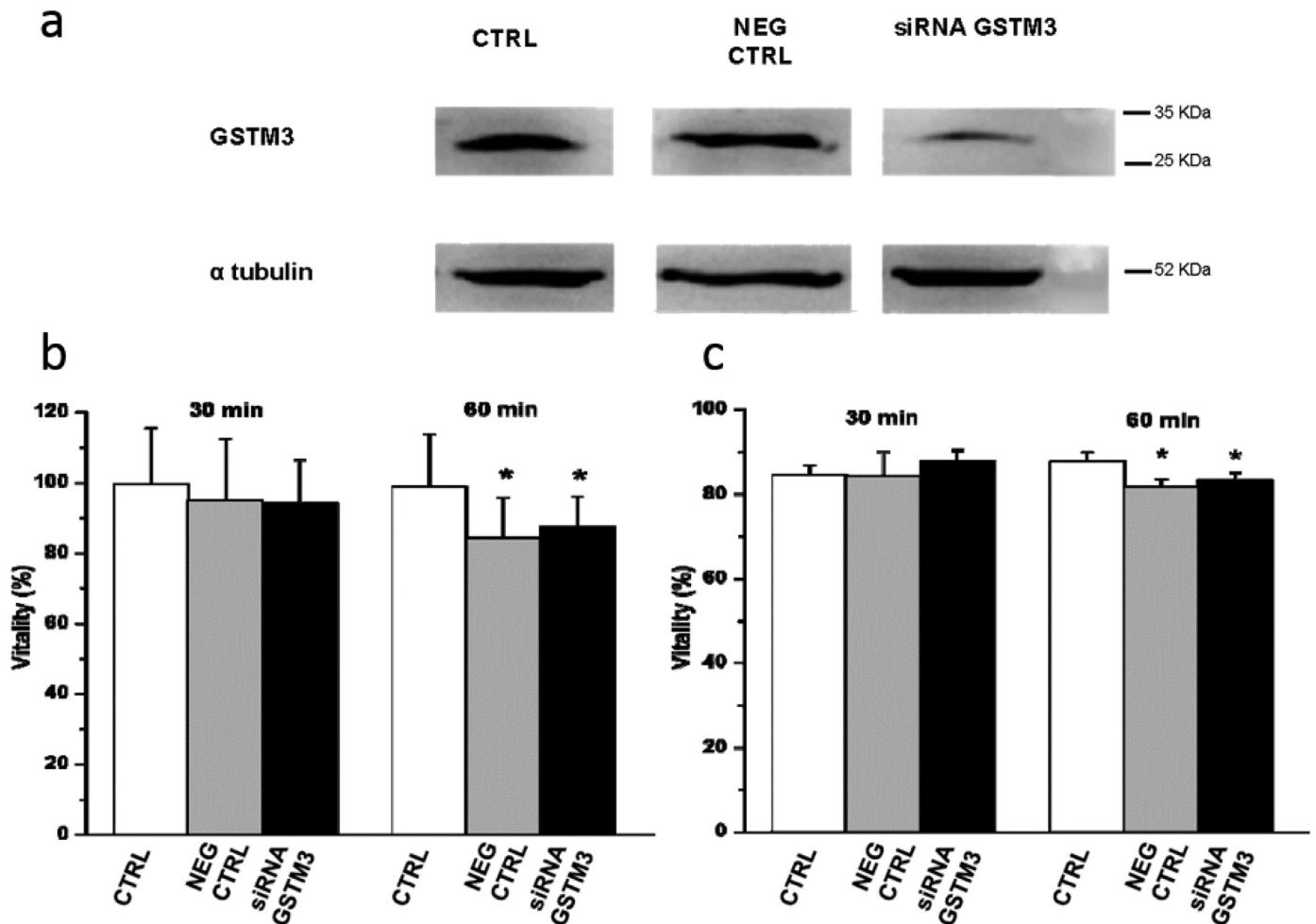


Fig. 3. *GSTM3* knockdown and its effects on cell cytotoxicity. (A) Results obtained from HEK Nav1.5 cells (CTRL), and cells transfected with a non-targeting siRNA (NEG CTRL) or siRNA specific for *GSTM3* (siRNA *GSTM3*), showing the *GSTM3* protein is down-regulated by about 50% (normalised to α -tubulin protein expression). Three different transfections and at least 3 different western blots were performed. (B and C) Bar graphs showing the results of the cytotoxicity tests (MTT and LDH, respectively). Y-axis represents the vitality of the cells incubated for 30 or 60 min with 15 mM tBHP. Data are presented as mean values \pm S.E. and were derived from at least 2 different experiments, each consisting of 6 different wells. * $P < 0.05$. (ANOVA, followed by a modified t-test with Fisher LSD correction).

TWB samples ($N = 15,829$). Intriguingly, the *GSTM3* deletion was not reported in the large dataset based on whole-genome sequences ($>10,000$ individuals), suggesting that it is closely associated with BrS.

The value of genetic variants as a tool to evaluate recurrent arrhythmic risk in BrS is still undetermined [1]. In this study, although not all BrS families showed complete co-segregation of the *GSTM3* deletion with BrS, the frequency of SCA in BrS patients with deletion of *GSTM3* was significantly higher than in BrS patients without the deletion, suggesting that the clinical presentation of BrS patients with the deletion of *GSTM3* may be more severe. We also observed that the frequency of VA was significantly higher in *GSTM3* knockout zebrafish than in WT zebrafish. In other words, our findings suggest that deletion of *GSTM3* may exert modulatory effect on arrhythmia risk in Taiwanese BrS patients, and provide a reference for risk stratification of BrS patients.

GSTM3 encodes a glutathione S-transferase involved in anti-oxidant defense, protecting the cells from oxidative stress [41]. The deleted region of *GSTM3* contains the 8th exon and the transcription stop site. Thus, this deletion may result in failed transcription termination, leading to nonsense-mediated degradation of *GSTM3* mRNA [42]. Cardiac oxidative stress caused by reactive oxygen species (ROS) has been demonstrated to play an important role in the mechanism

of cardiac arrhythmia and SCD [43,44]. In excitable cardiac cells, ROS regulate both cellular metabolism and ion homeostasis. Increasing evidence suggests that elevated cellular ROS can cause alterations of membrane current in isolated cardiac myocytes [45] and abnormal Ca^{2+} handling, leading to arrhythmogenesis [43]. In particular, ROS induce a reduction in the total cardiac sodium current and a leftward shift in the availability curve [34,45]. The pathogenic mechanism underlying BrS may involve an outward shift in the balance of current in the early phases of the action potential in the epicardium of the right ventricular outflow tract, secondary to a decrease in inward current (e.g., I_{Na}) or an increase in outward current (e.g., $I_{\text{K-ATP}}$). Oxidative stress, among other effects, produces both a decrease in I_{Na} and an increase in $I_{\text{K-ATP}}$. Our data from HEK293 Nav1.5 cells showed that, upon treatment with the direct-acting oxidative agent tBHP, the reduction in I_{Na} is amplified when *GSTM3* is reduced. A loss of I_{Na} has been shown to leave the transient outward current (I_{to}) less opposed, thus accentuating the epicardial action potential notch in the outflow tract of the right ventricle, leading to loss of the action potential dome and the development of phase 2 reentrant extra-systoles capable of precipitating VT/VF [46]. Reduced I_{Na} has also been proposed to contribute to the manifestation of BrS by slowing impulse conduction into the right ventricular outflow tract (RVOT) [47]. Our findings suggest that a decrease in *GSTM3* copy number can amplify the effect of

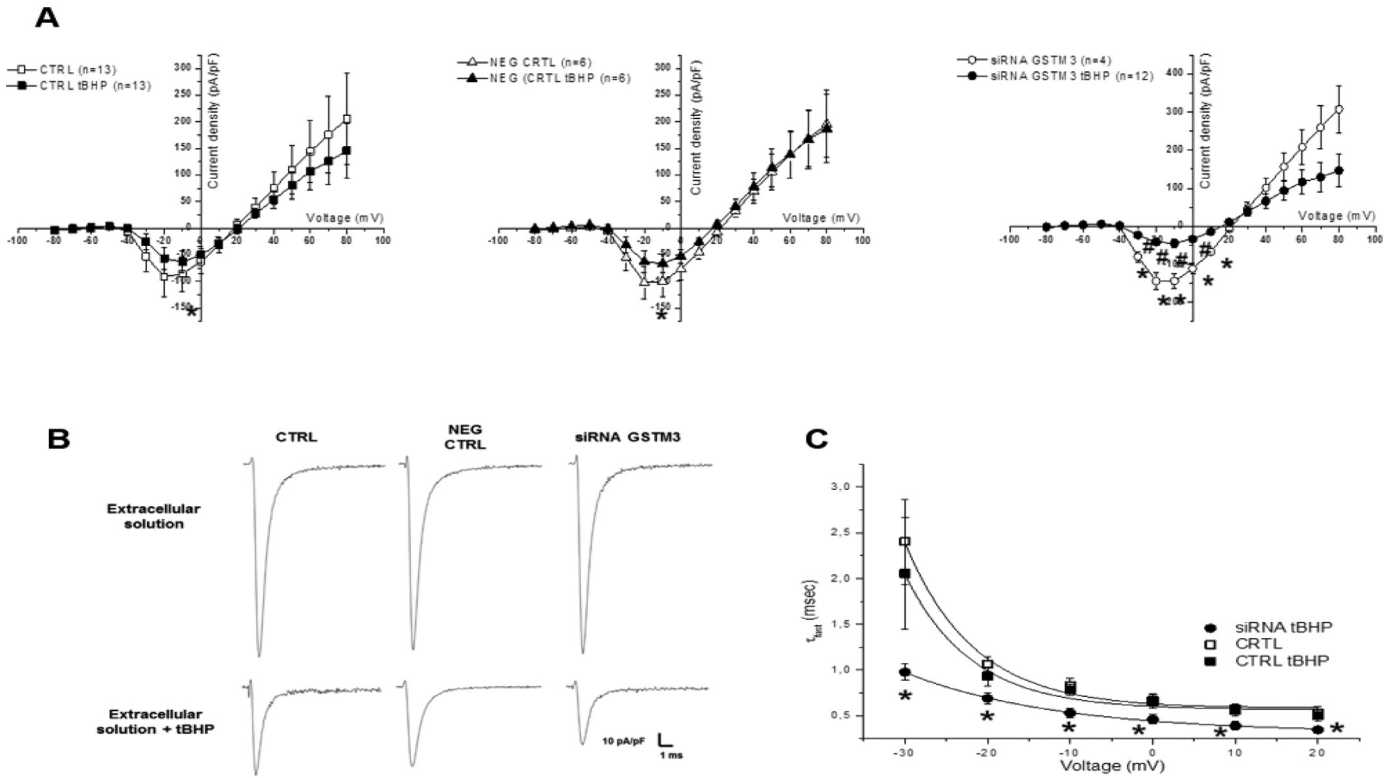


Fig. 4. Effect of tBHP on the Nav1.5 peak current density and kinetics of inactivation. (A) Current-voltage relationship of peak inward currents in HEK Nav1.5 cells (CTRL), in HEK Nav1.5 cells transfected with a non-targeting siRNA (NEG CTRL) or siRNA specific for GSTM3 (siRNA GSTM3) in the absence (empty symbols) or in presence (filled symbols) of tBHP. After performed multiple testing correction, * $P < 0.005$ vs the respective untreated condition; # $P < 0.005$ vs CTRL tBHP. In parentheses is the number of cells. (B) Peak currents evoked by a voltage step at -10 mV (holding potential -100 mV) normalised by cell capacitance, in the absence (upper traces) or presence (lower traces) of tBHP. (C) Kinetics of the onset of fast inactivation. * $P < 0.005$ after performed multiple testing correction. (ANOVA, followed by a modified t-test with Fisher LSD correction).

In Panel A and C, data are presented as mean values \pm S.E.

ROS to reduce I_{Na} , thus predisposing patients to the development of the BrS (Fig. 7). In the other hand, we found that $T_{peak-Tend}$ interval in *GSTM3* deletion group was statistically longer and had more episodes of SCA or syncope than that in no deletion group. Prolonged $T_{peak-Tend}$ interval, representing the dispersion of repolarization, has been reported as a risk factor for BrS [48-50]. Our findings were consistent with previous studies.

There are some limitations in this study. First, because this is not a prospective cohort study, we could not use the deletion of *GSTM3* to predict future ventricular events for asymptomatic BrS patients. Second, although our cellular and animal studies showed that deletion of *GSTM3* could alter electrophysiological stability and increase the frequency of VA, we cannot claim that this CNV is causal for BrS, because

it exists in approximately 0.1–0.8% of healthy controls. Third, we do not have other ethnic BrS DNA samples to test our findings, and further studies in different ethnicities are warranted to validate this *GSTM3* deletion. Lastly, we utilized two different experimental approaches to evaluate the segment of the *GSTM3* deletion in this study. Because both microarray and exome sequencing belong to high-throughput genomic technologies, their advantage is to perform a genome-wide screening of possible segments with CNV. Therefore, these two high-throughput methods may have relatively higher false negative rates due to the absence of specific probes or sequencing reads in the corresponding regions. Alternatively, Sanger sequencing uses primers designed specifically for the region of interest. Thus, Sanger sequencing may have relatively lower false negative rates.

Table 3

Properties of I_{Na} current in control and *GSTM3*-silenced cells in the presence or absence of 15 mM tBHP.

	Current density(pA/pF)		Activation Curve		Availability Curve	
			$V_{1/2}$ (mV)	k	$V_{1/2}^{(a)}$ (mV)	k
CTRL	-145.9 ± 24.3 (n = 44)		-24.3 ± 1.2 (n = 13)	7.5 ± 0.8	-64.0 ± 2.2 (n = 28)	8.4 ± 0.4
CTRL + tBHP	-55.3 ± 16.1 (n = 13)*		-21.6 ± 2.2 (n = 13)	9.1 ± 1.5	-72.5 ± 0.9 (n = 6)*	8.2 ± 0.7
NEG CTRL	-146.9 ± 21.9 (n = 23)		-24.1 ± 2.8 (n = 6)	6.8 ± 0.7	-67.0 ± 1.8 (n = 10)	7.8 ± 0.3
NEG CTRL + tBHP	-64.4 ± 21.9 (n = 18)*		-19.3 ± 2.8 (n = 6)	9.02 ± 1.1	-75.8 ± 2.8 (n = 15)*	7.4 ± 0.6
GSTM3 siRNA	-164.4 ± 32.0 (n = 20)		-20.8 ± 4.7 (n = 4)	8.06 ± 1.2	-64.4 ± 1.6 (n = 19)	8.2 ± 0.4
GSTM3 siRNA + tBHP	-41.4 ± 8.5 (n = 23)*, #		-22.8 ± 5.3 (n = 12)	8.07 ± 1.02	-82.8 ± 2.6 (n = 7)*, #, §	7.02 ± 0.2

$V_{1/2}$, voltage of half-maximal activation; $V_{1/2}^{(a)}$, prepulse voltage where half-maximal inactivation occurred; k, slope factor. CTRL, untransfected cells; NEG CTRL, cells transfected with non-targeting siRNA. Values are means \pm SE. n is the number of cells patched from at least three different experiments. * $P < 0.005$ vs. the respective tBHP untreated condition; # $P < 0.005$ vs CTRL + tBHP; § $P < 0.005$ vs NEG CTRL + tBHP. (ANOVA, followed by a modified t-test with Fisher LSD correction).

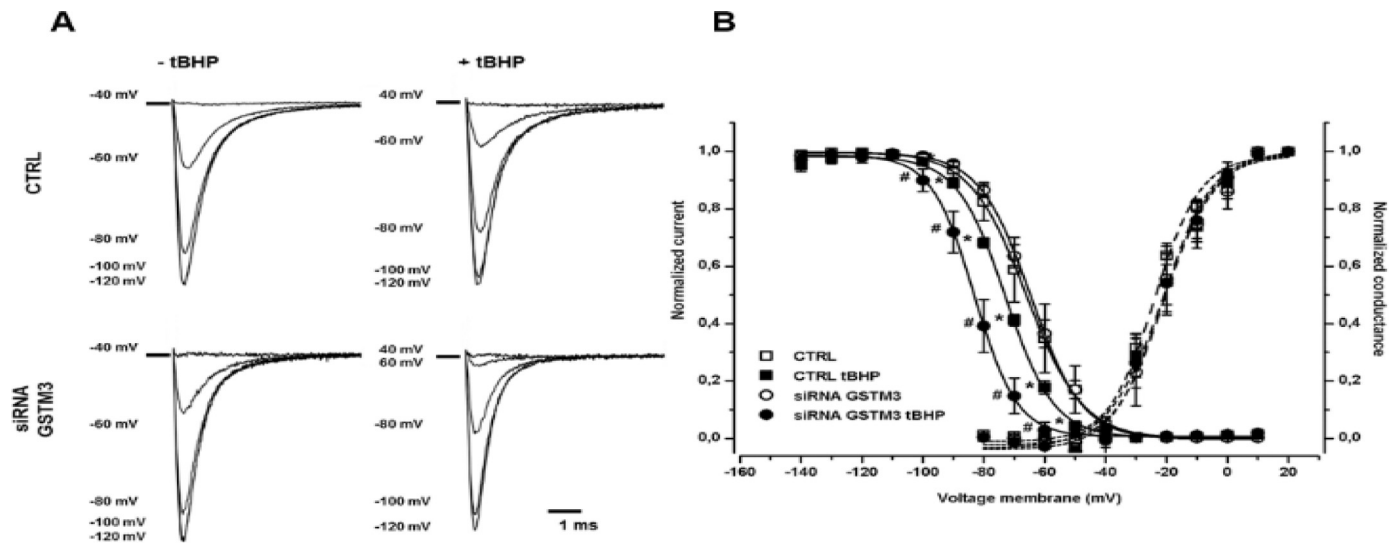


Fig. 5. Effect of tBHP on Nav1.5 activation curve and channel availability. (A) Families of current traces recorded in HEK Nav1.5 cells (CTRL) and in HEK Nav1.5 cells with *GSTM3* silenced (siRNA *GSTM3*), at selected voltages in the absence (-tBHP) or presence (+tBHP) of tBHP. (B) The silencing of *GSTM3* had no effect on the availability curves (solid lines) (CTRL vs siRNA *GSTM3*, open squares vs open circles). tBHP (15 mM) induced a hyperpolarizing shift in the $V_{1/2}$ of -8.5 mV in HEK Nav1.5 cells (CTRL vs CTRL tBHP; open squares vs filled squares) and of -18.4 mV when *GSTM3* was silenced (siRNA *GSTM3* vs siRNA *GSTM3* tBHP; open circles vs filled circles). No significant differences were observed in the activation properties (dashed lines). Results from the NEG CTRL cell line were omitted for the sake of clarity.

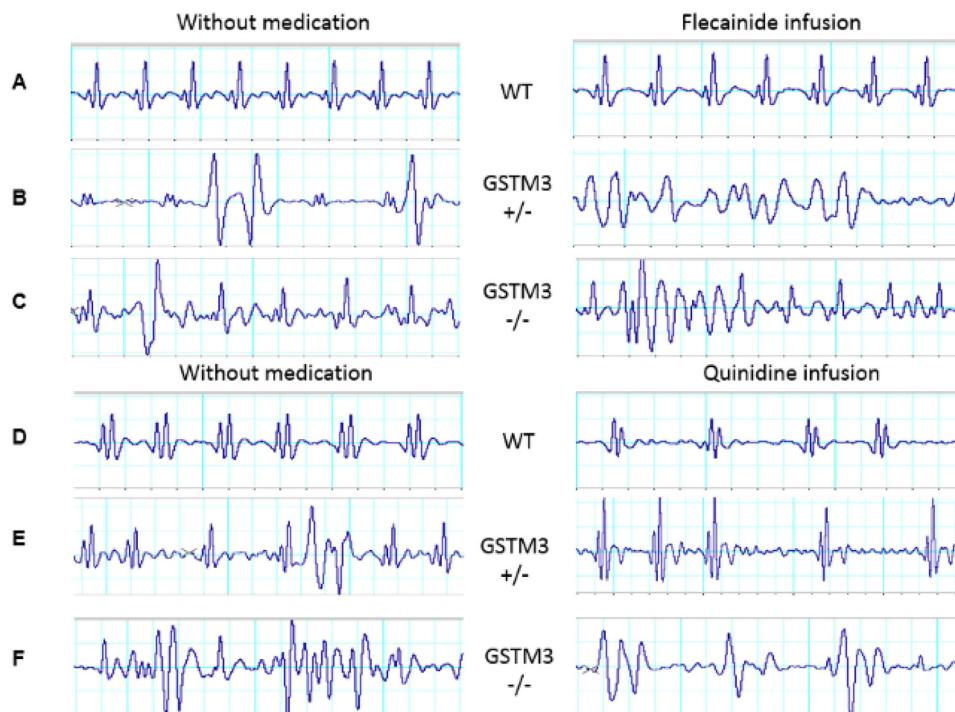


Fig. 6. An example of ventricular arrhythmia in WT, *GSTM3*^{+/-}, and *GSTM3*^{-/-} adult zebrafish recorded by a surface ECG system. Arrhythmic activities shown here were selected from experiments with $10 \mu\text{M}$ flecainide (A-C) and $0.1 \mu\text{M}$ quinidine (D-F). These representative ECG traces illustrate the ventricular arrhythmia of WT and *GSTM3* knockout fish before and after administrating flecainide and quinidine.

In terms of clinical implications, our study identified a deletion of *GSTM3* in BrS patients, which is associated with reduced I_{Na} , suggesting that the deletion could be a genetic modifier of the BrS phenotype. In addition, it could be used as a risk predictor in patients with BrS.

Funding sources

This research was partially supported by grants NTUH 106-S3469, NTUH 105-012, UN 103-018, and UN104-001 from National Taiwan

University Hospital (to JMJJ); NSC 101-2314-B-002-168-MY2, NSC 103-2314-B-002-148, MOST 104-2314-B-002-193-MY3, MOST 106-2314-B-002-047-MY3, MOST 106-2314-B-002-206, MOST 107-2314-B-002-009, MOST 107-2314-B-002-007, MOST 108-2314-B-002-007 and MOST 107-2314-B-002-261-MY3 from the Ministry of Science and Technology (to JMJJ), Taiwan Health Foundation (to JMJJ); NTU CESRP-10R70602A5 and NTU ERP-10R80600 from National Taiwan University (to SJL), grant GTZ300 from National Taiwan University (to TPL and EYC); grants HL47678, HL138103 and HL152201 from the National Institutes of Health, U.S.A. (to CA); grant H1802

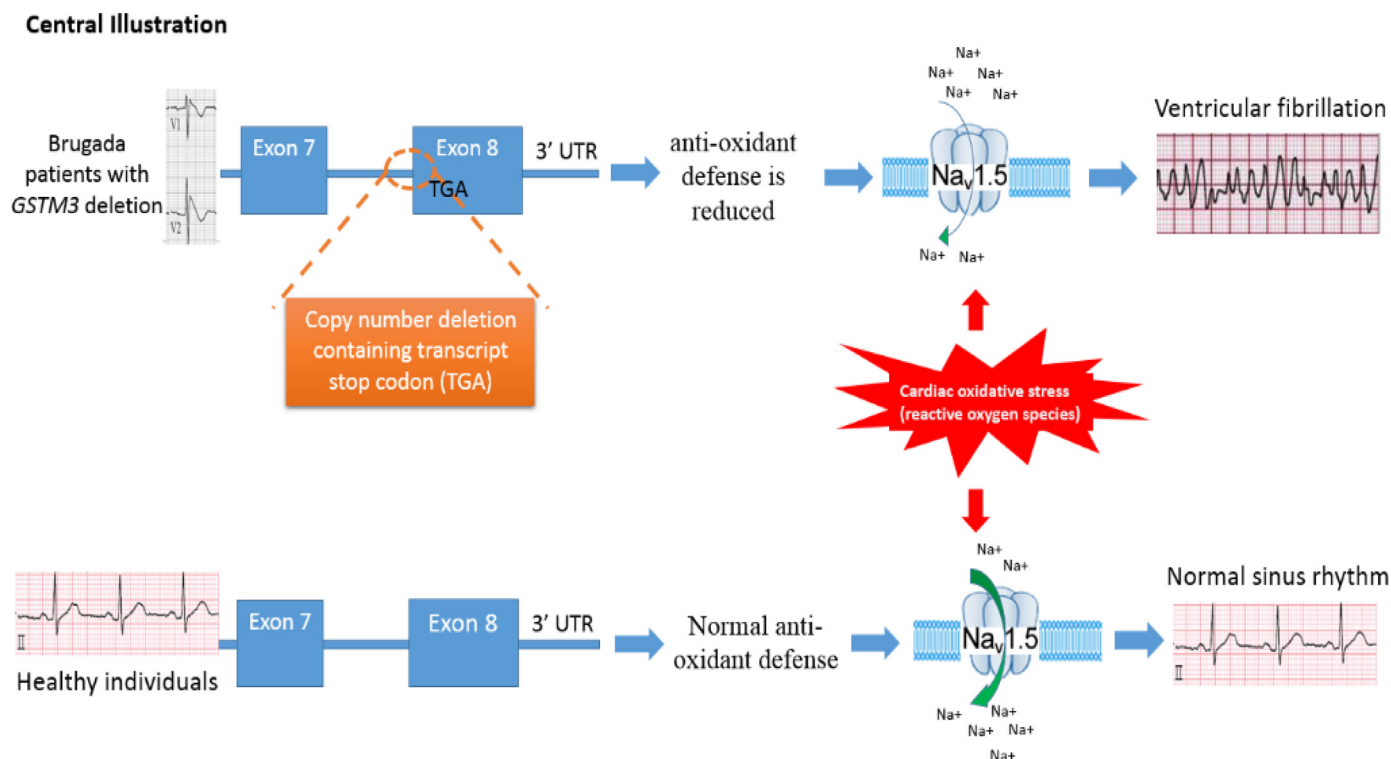


Fig. 7. *GSTM3* deletion reduces antioxidant defense, thus increasing vulnerability of Brugada syndrome patients to development of life-threatening ventricular arrhythmias under conditions of oxidative stress. Failed transcription termination is thought to lead to nonsense-mediated degradation of *GSTM3* mRNA, resulting in reduced levels of glutathione S-transferase and an inability to protect against the effects of reactive oxygen species, namely the reduction of cardiac sodium channel current density and precipitation of VT/VF.

from the W.W. Smith Charitable Trust (to CA); and the Martha and Wistar Morris Fund, U.S.A (to CA). Support for IR was from grant 2016-ATE-0292 from the Fondo Ateneoper la Ricerca, Italy. All funders had no role in study design, data collection, data analysis, interpretation, and writing of the manuscript. CA and TPL had full access to all the data in the study and had final responsibility for the decision to submit for publication. All authors declared no competing financial interests.

Declarations of Competing Interest

The authors declared that they have no conflict of interests.

Acknowledgements

We are sincerely grateful to many cardiologists, including Dr. Shoei K. Stephen Huang, Dr. Tsu-Juey Wu, Dr. Chun-Chieh Wang, Dr. Kuan-Cheng Chang, Dr. Meng-Huan Lei, Dr. An-Ning Feng, Dr. Wen-Chin Ko, Dr. Jin-Long Huang, Dr. Wen-Chin Tsai, Dr. Huey-Ming Lo, Dr. Jen-Fu Liu, Dr. Ying-Chieh Liao, Dr. Mei-Hwan Wu, Dr. Ming-Tai Lin, Dr. Shuenn-Nan Chiu, Dr. Su-Kiat Chua, RN Fu-Lan Chang, and many other doctors in other medical centers or hospitals, for referring patients to our hospital, and to the staff of the Sixth Core Lab of NTUH and the Zebrafish Core facility of National Taiwan University for technical support. We also acknowledge Dr. Hugues Abriel for the HEK293 cell line, Ms. Yi-Yu Su, and the technical/bioinformatics services provided by the National Center for Genome Medicine of the National Core Facility Program for Biotechnology, Ministry of Science and Technology. We thank Melissa Stauffer, Ph.D., for editing the manuscript.

Supplementary materials

Supplementary material associated with this article can be found, in the online version, at [doi:10.1016/j.ebiom.2020.102843](https://doi.org/10.1016/j.ebiom.2020.102843).

References

- [1] Mizusawa Y, Wilde AA. Brugada syndrome. *Circ Arrhythm Electrophysiol* 2012;5(3):606–16.
- [2] Juang JM, Chen CY, Chen YH, et al. Prevalence and prognosis of Brugada electrocardiogram patterns in an elderly Han Chinese population: a nation-wide community-based study (HALST cohort). *Europace* 2015;17(Suppl 2):ii54–62.
- [3] Juang JM, Huang SK, Tsai CT, et al. Characteristics of Chinese patients with symptomatic Brugada syndrome in Taiwan. *Cardiology* 2003;99(4):182–9.
- [4] Priori SG, Wilde AA, Horie M, et al. Executive summary: HRS/EHRA/APHS expert consensus statement on the diagnosis and management of patients with inherited primary arrhythmia syndromes. *Europace* 2013;15(10):1389–406.
- [5] Juang JM, Tsai CT, Lin LY, et al. Unique clinical characteristics and SCN5A mutations in patients with Brugada syndrome in Taiwan. *J Formos Med Assoc* 2015;114(7):620–6.
- [6] Juang JJ, Horie M. Genetics of Brugada syndrome. *J Arrhythm* 2016;32(5):418–25.
- [7] Juang JM, Lu TP, Lai LC, et al. Disease-targeted sequencing of ion channel genes identifies de novo mutations in patients with non-familial Brugada syndrome. *Sci Rep* 2014;4:6733.
- [8] Bezzina CR, Barc J, Mizusawa Y, et al. Common variants at SCN5A-SCN10A and HEY2 are associated with Brugada syndrome, a rare disease with high risk of sudden cardiac death. *Nat Genet* 2013;45(9):1044–9.
- [9] Pollex RL, Hegele RA. Copy number variation in the human genome and its implications for cardiovascular disease. *Circulation* 2007;115(24):3130–8.
- [10] Soemedi R, Wilson IJ, Bentham J, et al. Contribution of global rare copy-number variants to the risk of sporadic congenital heart disease. *Am J Hum Genet* 2012;91(3):489–501.
- [11] Li D, Lewinger JP, Gauderman WJ, Murcay CE, Conti D. Using extreme phenotype sampling to identify the rare causal variants of quantitative traits in association studies. *Genet Epidemiol* 2011;35(8):790–9.
- [12] Barnett IJ, Lee S, Lin X. Detecting rare variant effects using extreme phenotype sampling in sequencing association studies. *Genet Epidemiol* 2013;37(2):142–51.
- [13] Wu CK, Juang JJ, Chiang JY, Li YH, Tsai CT, Chiang FT. The Taiwan heart registries: its influence on cardiovascular patient care. *J Am Coll Cardiol* 2018;71(11):1273–83.

- [14] Antzelevitch C, Yan GX, Ackerman MJ, et al. J-Wave syndromes expert consensus conference report: emerging concepts and gaps in knowledge. *Heart Rhythm* 2016;13(10):e295–324.
- [15] Wang Q, Li Z, Shen J, Keating MT. Genomic organization of the human SCN5A gene encoding the cardiac sodium channel. *Genomics* 1996;34(1):9–16.
- [16] Richards S, Aziz N, Bale S, et al. Standards and guidelines for the interpretation of sequence variants: a joint consensus recommendation of the American college of medical genetics and genomics and the association for molecular pathology. *Genet Med* 2015;17(5):405–24.
- [17] Juang JM, Phan WL, Chen PC, et al. Brugada-type electrocardiogram in the Taiwanese population—is it a risk factor for sudden death? *J Formos Med Assoc* 2011;110(4):230–8.
- [18] Mills KT, Bundy JD, Kelly TN, et al. Global disparities of hypertension prevalence and control: a systematic analysis of population-based studies from 90 countries. *Circulation* 2016;134(6):441–50.
- [19] Grayson BL, Aune TM. A comparison of genomic copy number calls by Partek Genomics Suite, Genotyping Console and Birdsuite algorithms to quantitative PCR. *BioData Min* 2011;4:8.
- [20] Talevich E, Shain AH, Botton T, Bastian BC. CNVkit: genome-wide copy number detection and visualization from targeted DNA sequencing. *PLoS Comput Biol* 2016;12(4):e1004873.
- [21] Hirschhorn JN, Daly MJ. Genome-wide association studies for common diseases and complex traits. *Nat Rev Genet* 2005;6(2):95–108.
- [22] Antzelevitch C, Yan GX, Ackerman MJ, et al. J-Wave syndromes expert consensus conference report: emerging concepts and gaps in knowledge. *Europace* 2017;19(4):665–94.
- [23] Fagerberg L, Hallström BM, Oksvold P, et al. Analysis of the human tissue-specific expression by genome-wide integration of transcriptomics and antibody-based proteomics. *Mol Cell Proteom* 2014;13(2):397–406.
- [24] Panariti A, Lettiero B, Alexandrescu R, et al. Dynamic investigation of interaction of biocompatible iron oxide nanoparticles with epithelial cells for biomedical applications. *J Biomed Nanotechnol* 2013;9(9):1556–69.
- [25] Bugiardini E, Rivolta I, Binda A, et al. SCN4A mutation as modifying factor of myotonic dystrophy type 2 phenotype. *Neuromuscul Disord* 2015;25(4):301–7.
- [26] Rivolta I, Clancy CE, Tateyama M, Liu H, Priori SG, Kass RS. A novel SCN5A mutation associated with long QT-3: altered inactivation kinetics and channel dysfunction. *Physiol Genom* 2002;10(3):191–7.
- [27] Livak KJ, Schmittgen TD. Analysis of relative gene expression data using real-time quantitative PCR and the 2(-Delta Delta C(T)) Method. *Methods* 2001;25(4):402–8.
- [28] Priori SG, Wilde AA, Horie M, et al. HRS/EHRA/APHRS expert consensus statement on the diagnosis and management of patients with inherited primary arrhythmia syndromes: document endorsed by HRS, EHRA, and APHRS in May 2013 and by ACCF, AHA, PACES, and AEPC in June 2013. *Heart Rhythm* 2013;10(12):1932–63.
- [29] Chopra SS, Stroud DM, Watanabe H, et al. Voltage-gated sodium channels are required for heart development in zebrafish. *Circ Res* 2010;106(8):1342–50.
- [30] Rahm A-K, Wiedmann F, Gierten J, et al. Functional characterization of zebrafish K2P18.1 (TRESK) two-pore-domain K⁺ channels. *Naunyn Schmiedeberg Arch Pharmacol* 2014;387(3):291–300.
- [31] Stokoe KS, Balasubramaniam R, Goddard CA, Colledge WH, Grace AA, Huang CL. Effects of flecainide and quinidine on arrhythmogenic properties of Scn5a^{+/-} murine hearts modelling the Brugada syndrome. *J Physiol* 2007;581(Pt 1):255–75.
- [32] Uchida T, Nishimura M, Saeki T, Watanabe Y. Effects of membrane lipid peroxidation by tert butyl hydroperoxide on the sodium current in isolated feline ventricular myocytes. *Heart Vessels* 1994;9(5):227–34.
- [33] Barrington PL, Martin RL, Zhang K. Slowly inactivating sodium currents are reduced by exposure to oxidative stress. *J Mol Cell Cardiol* 1997;29(12):3251–65.
- [34] Fukuda K, Davies SS, Nakajima T, et al. Oxidative mediated lipid peroxidation recapitulates proarrhythmic effects on cardiac sodium channels. *Circ Res* 2005;97(12):1262–9.
- [35] Nakajima T, Davies SS, Matafonova E, et al. Selective gamma-ketoaldehyde scavengers protect Nav1.5 from oxidant-induced inactivation. *J Mol Cell Cardiol* 2010;48(2):352–9.
- [36] Eastaugh LJ, James PA, Phelan DG, Davis AM. Brugada syndrome caused by a large deletion in SCN5A only detected by multiplex ligation-dependent probe amplification. *J Cardiovasc Electrophysiol* 2011;22(9):1073–6.
- [37] Koopmann TT, Beekman L, Alders M, et al. Exclusion of multiple candidate genes and large genomic rearrangements in SCN5A in a Dutch Brugada syndrome cohort. *Heart Rhythm* 2007;4(6):752–5.
- [38] Mademont-Soler I, Pinsach-Abuin ML, Riuro H, et al. Large genomic imbalances in Brugada syndrome. *PLoS ONE* 2016;11(9):e0163514.
- [39] García-Molina E, Lacunza J, Ruiz-Espejo F, et al. A study of the SCN5A gene in a cohort of 76 patients with Brugada syndrome. *Clin Genet* 2013;83(6):530–8.
- [40] Sonoda K, Ohno S, Ozawa J, et al. Copy number variations of SCN5A in Brugada syndrome. *Heart Rhythm* 2018;15(8):1179–88.
- [41] Hayes JD, McLellan LL. Glutathione and glutathione-dependent enzymes represent a co-ordinately regulated defence against oxidative stress. *Free Radic Res* 1999;31(4):273–300.
- [42] Hentze MW, Kulozik AE. A perfect message: RNA surveillance and nonsense-mediated decay. *Cell* 1999;96(3):307–10.
- [43] Jeong EM, Liu M, Sturdy M, et al. Metabolic stress, reactive oxygen species, and arrhythmia. *J Mol Cell Cardiol* 2012;52(2):454–63.
- [44] Sovari AA, Rutledge CA, Jeong EM, et al. Mitochondria oxidative stress, connexin43 remodeling, and sudden arrhythmic death. *Circ Arrhythm Electrophysiol* 2013;6(3):623–31.
- [45] Bhatnagar A, Srivastava SK, Szabo G. Oxidative stress alters specific membrane currents in isolated cardiac myocytes. *Circ Res* 1990;67(3):535–49.
- [46] Antzelevitch C, Yan GX, Ackerman MJ, et al. J-Wave syndromes expert consensus conference report: emerging concepts and gaps in knowledge. *J Arrhythm* 2016;32(5):315–39.
- [47] Wilde AA, Postema PG, Di Diego JM, et al. The pathophysiological mechanism underlying Brugada syndrome: depolarization versus repolarization. *J Mol Cell Cardiol* 2010;49(4):543–53.
- [48] Tse G, Gong M, Wong WT, et al. The Tpeak - Tend interval as an electrocardiographic risk marker of arrhythmic and mortality outcomes: a systematic review and meta-analysis. *Heart Rhythm* 2017;14(8):1131–7.
- [49] Tse G, Gong M, Li CKH, et al. Tpeak-Tend, Tpeak-Tend/QT ratio and Tpeak-Tend dispersion for risk stratification in Brugada Syndrome: a systematic review and meta-analysis. *J Arrhythm* 2018;34(6):587–97.
- [50] Tse G, Yan BP. Traditional and novel electrocardiographic conduction and repolarization markers of sudden cardiac death. *EP Europace* 2016;19(5):712–21.